approximately parallel in adjacent molecules. The other phenyl ring has near-neighbour phenyl rings which are roughly perpendicular to it. Table 6 contains the shorter non-bonded contacts of O(16) and O(17). The outstanding feature is that O(16) has contacts with C(4), C(5) and C(6) of an adjacent molecule which are just greater than van der Waals contacts. Hence the environment in the vicinity of the hydrogen bond is asymmetric.

This 1,3-diketone is symmetrically substituted in the 1- and 3-positions. It might be expected that an equilibrium mixture of the two possible enol tautomers would result. The inequality in the bond lengths of the pairs C(13)–C(14), C(14)–C(15) and C(13)–O(16), C(15)–O(17) is not consistent with such a description. For a unique enol, the values of these bond lengths would be approximately 1·47, 1·33 and 1·2, 1·4 Å. If the final atomic positions obtained represented an average of the two enol tautomers, and any other combinations which might arise due to packing in the crystal, large thermal motion would be expected along the bond directions. This was not evident before or after correction for rigid-body motion. Our evidence, therefore, suggests a unique enol form which has been distorted by an asymmetric environment.

For the duration of this work, the author had tenure of an Australian Institute of Nuclear Science and Engineering Research Fellowship.

References

ABRAHAMS, S. C. & KEVE, E. T. (1971). *Acta Cryst.* A**27**, 157–163.

BACON, G. E. (1972). *Acta Cryst.* A**28**, 357–358.

BUSING, W. R. & LEVY, H. A. (1964). *Acta Cryst.* **17**, 142–146.

COPPENS, P. & HAMILTON, W. C. (1970). *Acta Cryst.* A**26**, 71–83.

ELCOMBE, M. M., COX, G. W., PRYOR, A. W. & MOORE, F. H. (1971). *Programs for the Management and Processing of Neutron Diffraction Data.* Report AAEC/TM578, Australian Atomic Energy Commission.

FINHOLT, J. E. & WILLIAMS, J. M. (1973). *J. Chem. Phys.* **59**, 5114–5121.

HAMILTON, W. C. & ABRAHAMS, S. C. (1972). *Acta Cryst.* A**28**, 215–218.

HOLLANDER, F. J., TEMPLETON, D. H. & ZALKIN, A. (1973). *Acta Cryst.* B**29**, 1552–1553.

MACDONALD, A. L. & SPEAKMAN, J. C. (1972). *J. Chem. Soc. Perkin* II, pp. 825–832.

MOORE, F. H. (1972). *Acta Cryst.* A**28**, S256.

SCHLEMPER, E. O., HAMILTON, W. C. & LA PLACA, S. J. (1971). *J. Chem. Phys.* **54**, 3990–4000.

SCHOMAKER, V. & TRUEBLOOD, K. N. (1968). *Acta Cryst.* B**24**, 63–76.

SEQUEIRA, A., BERKEBILE, C. A. & HAMILTON, W. C. (1967). *J. Mol. Struct.* **1**, 283–294.

WILLIAMS, D. E. (1966). *Acta Cryst.* **21**, 340–349.

WILLIAMS, J. M. (1974). *Diffraction Studies of Real Atoms and Real Crystals.* Abstract I K-3, Int. Crystallogr. Conf., Melbourne.

Acta Cryst. (1976). B**32**, 1811

Structures of Uranyl-Decorated Lecithin and Lecithin–Cholesterol Bilayers

BY KISHIO FURUYA, TAKASHI YAMAGUCHI,* YŌJI INOKO AND TOSHIO MITSUI

Department of Biophysical Engineering, Faculty of Engineering Science, Osaka University, Toyonaka, Osaka 560, *Japan*

(*Received* 19 *July* 1975; *accepted* 4 *November* 1975)

Dipalmitoyl lecithin and dipalmitoyl lecithin–cholesterol bilayers are capable of binding about the same number of uranyl ions as lecithin molecules. Dispersions of the uranyl-decorated bilayers give very distinct continuous X-ray diffraction peaks up to the seventh order. Electron density projection onto the normal to the membrane is obtained with a resolution of about 6·5 Å. It gives two high peaks separated by 48 Å indicating that uranyl ions are bound at the surfaces of membranes in both lecithin and lecithin–cholesterol bilayers.

Introduction

Uranyl acetate has been widely used as a stain in electron microscopy to investigate the structure of biomembranes. Shah (1969) studied the interaction of uranyl ions with phospholipid monolayers, and concluded that uranyl acetate does not cause degradation of phospholipids and stabilizes the monolayer films. Recently we have shown that adding a very small amount of uranyl acetate to the dipalmitoyl lecithin–water system destroys the lamellar phase and results in dispersion of lecithin membranes (Inoko, Yamaguchi, Furuya & Mitsui, 1975). During the experiments we found that the dispersions of lecithin and lecithin–cholesterol membranes decorated by about equimolar

* Present address: Institute of Basic Medicine, University of Tsukuba, Niihari-gun, Ibaragi 300-31, Japan.

uranyl acetate gave very distinct continuous X-ray diffraction patterns. In the present work these patterns have been studied in detail and sites of uranyl ions have been located in the membranes.

Experimental

Synthetic β,γ-dipalmitoyl-D,L-(α)-lecithin was purchased from Sigma Chemical Co. and cholesterol from Nakarai Chemicals, Ltd. They were used without further purification. Lecithin and cholesterol were respectively dissolved in chloroform and stored at −20°C. These solutions were mixed at the desired molar ratio of lecithin and cholesterol. The mixtures were dried and then kept in an evacuated desiccator for at least an hour. The dried lipids were then dispersed in a solution of uranyl acetate to produce lipid bilayers decorated by uranyl ions.

The amount of uranyl acetate dissolved in water can be measured by its strong absorption around 4300 Å. Fig. 1 demonstrates estimation of uranyl-bindings by membranes. Curve (*a*) gives the optical absorption of uranyl acetate solution in the absence of lipid bilayers as a standard. The dispersion of membranes forms a pellet at the bottom of a test tube. In Fig. 1 the circles stand for optical absorbance of the supernatant of the lecithin–water system and the crosses are for the lecithin–cholesterol–water system in which the molar ratio of cholesterol/lecithin was 15/85. In these measurements the amounts of water and lecithin were kept constant. In Fig. 1 the circles and crosses lie along the same curve (*b*). This fact implies that uranyl ions do not bind to cholesterol and also that the presence of cholesterol does not affect the affinity of uranyl ions to lecithin molecules. Curve (*b*) approaches asymptotically the dashed straight line, which crosses the abscissa at about 1·2, indicating that the uranyl ions can bind to lecithin molecules up to a roughly equimolar ratio.

The pellet of membrane dispersion was picked up and pressed into a thin-walled glass capillary having the internal diameter of 1·0 mm. The capillary was sealed and used for X-ray measurements. Diffraction patterns were recorded on Fuji Medical X-ray films, using an Elliott toroidal camera or a Franks point focusing camera, operated *in vacuo* to eliminate air scatterings. Cu *Kα* radiation ($\lambda = 1{\cdot}542$ Å) was used and diffraction spacings were calibrated with the sodium myristate powder pattern. Scattering intensities were obtained from densitometer tracings of diffraction photographs with correction for non-linearity between the intensity and the photographic density. All X-ray experiments were carried out at room temperature (20 ± 2°C).

Fig. 2(*a*) shows a diffraction pattern by the dispersion of lecithin membranes decorated by equimolar uranyl ions. Unlike the lamellar diffraction patterns, the peaks are continuous. They are, however, very distinct and could be recognized up to the seventh order on the original film. Less distinct diffuse peaks were observed for dispersions of membranes decorated by smaller numbers of uranyl ions. All these peaks could be indexed approximately by a single parameter D, as was demonstrated for other membrane dispersions by Wilkins, Blaurock & Engelman (1971). D increases with the molar ratio of uranyl acetate/lecithin: $D \approx 43$ Å at 3/100, 45 Å at 1/10, 47 Å at 1/2, 48·8 Å at 1/1. The distinctness of the peaks increases with increasing uranyl acetate: only three peaks could be recognized at the molar ratio of uranyl acetate/lecithin of 1/100, whereas seven peaks could be observed at 1/1. The spacings corresponding to these third and seventh peaks were 12 Å and 6·5 Å, respectively.

On addition of uranyl acetate the lecithin–cholesterol–water systems are affected similarly to the lecithin–water systems. Fig. 2(*b*) shows a diffraction pattern by the dispersion of the membranes, in which the molar ratio of cholesterol/lecithin was 15/85, which were decorated by uranyl ions equimolar to lecithin molecules. The vertical in Fig. 2(*b*) is parallel to the axis of the capillary tube. As exemplified by this figure, the system containing cholesterol often gave diffraction patterns which indicated preferred orientation of mem-

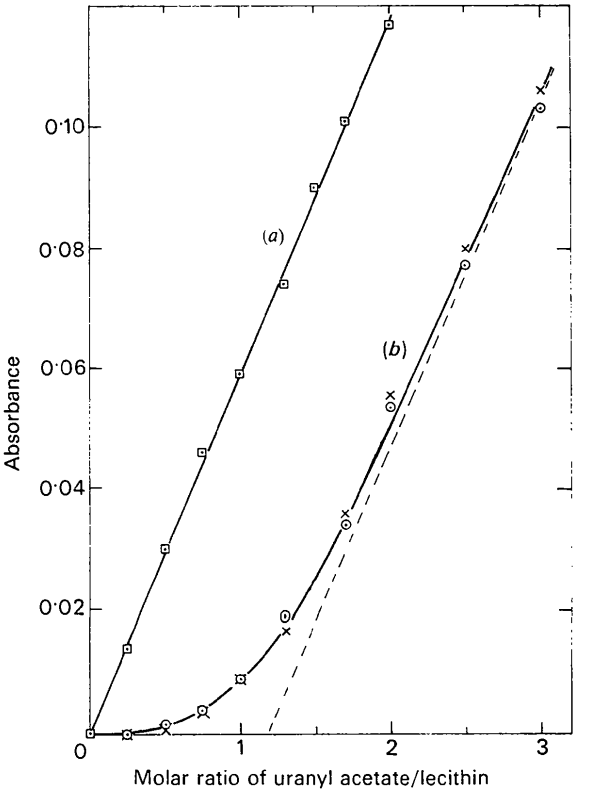

Fig. 1. Estimation of uranyl-bindings by membranes. Ordinate gives absorbance at 4300 Å. ⊡, control, absorbance measured in the absence of lipid membranes; ⊙, absorbance of supernatant of lecithin–water system; ×, absorbance of supernatant of lecithin–cholesterol–water system with a molar ratio of cholesterol/lecithin of 15/85.

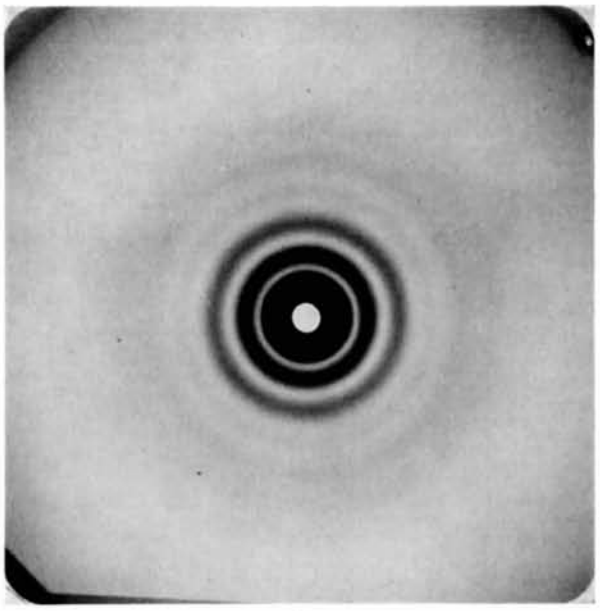

(*a*)

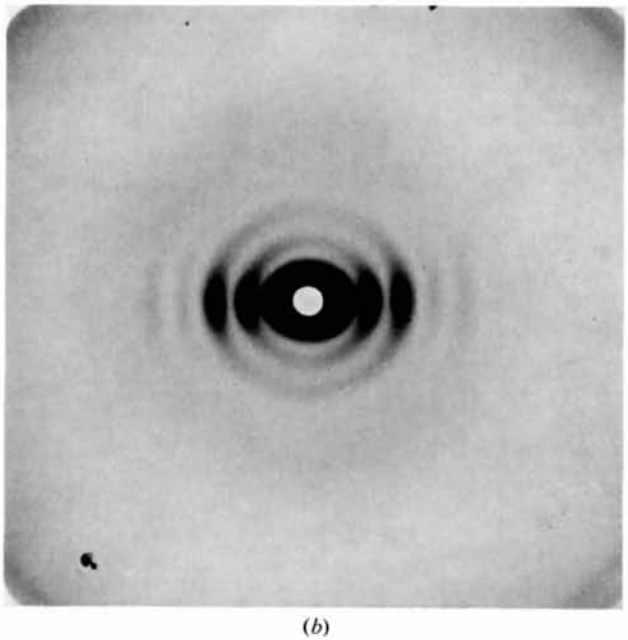

(*b*)

Fig. 2. X-ray diffraction patterns from dispersions of membranes which were decorated by uranyl acetate equimolar to lecithin. The vertical is parallel to the axis of the capillary tube which contains the dispersion. (*a*) lecithin bilayers (*L*); (*b*) lecithin–cholesterol bilayers with the molar ratio of cholesterol/lecithin of 15/85 (*LC*).

[*To face p.* 1812

branes in the capillary tube. Hereafter, for brevity, we shall call the specimens which gave the diffraction patterns shown in Fig. 2(*a*) and (*b*) as *L* and *LC*, respectively.

The high-angle (~4·2 Å) ring-like reflexion appeared in all original films, indicating an approximately crystalline packing of hydrocarbon chains in the membranes. It exhibited maximum intensity in the direction parallel to the capillary tube when the preferred orientation took place. This fact implies that the preferred orientation represents a tendency for the membranes to be parallel to the axis of the capillary tube.

Scattered X-ray intensities were determined by measuring densities of the films. The solid lines in Fig. 3(*a*) and (*b*) show the intensities along the horizontal lines passing through the centres of Fig. 2(*a*) and (*b*), respectively. The dashed curves are smoothly drawn backgrounds. Effects of parasitic scatterings were checked by using both Elliott and Franks cameras. Results proved that they only affected the background

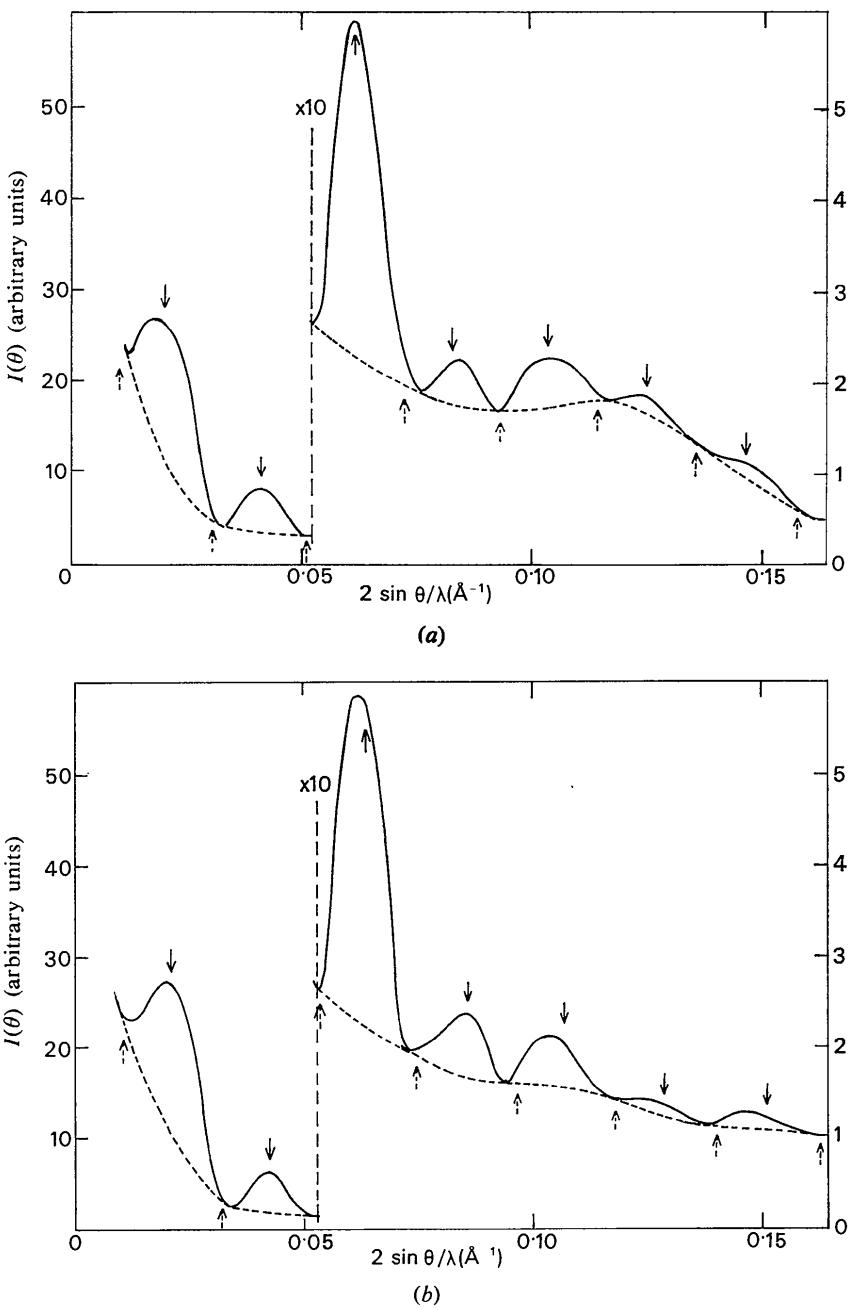

Fig. 3. Densities of the photographs shown in Fig. 2. The dashed curves show the backgrounds. Solid-line arrows show calculated maxima and dashed-line arrows minima (see text). (*a*) *L*; (*b*) *LC*.

at low angles. In Fig. 3(*a*), a broad peak can be seen in this background around 0·12 Å^{-1} of 2 sin θ/λ. A similar peak appears in Fig. 3(*b*), but its intensity is much less than that in Fig. 3(*a*). The original film of Fig. 2(*b*) showed that the broad peak corresponded to a part of a ring-like halo which has more intensity in the vertical direction than in the horizontal. Other photographs also showed that the intensity of the halo increases in the vertical direction relative to that in the horizontal with increasing degree of preferred orientation.

Structure analysis

Let us imagine a flat sheet of membrane in water. The Cartesian coordinates x, y are set in the plane of the membrane and z perpendicular to it. The corresponding coordinates in reciprocal space are denoted as X, Y and Z. The following symbols will be used: $\varrho(z)$, projection of the electron density of the membrane onto the z axis; ϱ_w, the electron density of water; $I(X,Y,Z)$, the intensity distribution of scattered X-rays by the single membrane; $I(Z)\equiv I(0,0,Z)$, the intensity distribution along the Z axis; $F(Z)$, the scattering amplitude along the Z axis in e Å^{-2}; $F_o(Z)$, the observed scattering amplitude. The density $\varrho(z)$ is expected to be an even function of z, and thus we have:

$$\varrho(z)-\varrho_w=2\int_0^\infty F(Z)\cos(2\pi Zz)\,\mathrm{d}Z; \qquad (1)$$

$$|F(Z)|^2=I(Z)\,. \qquad (2)$$

We make the following assumptions to obtain $F(Z)$: (1) the data presented in Fig. 3 contain no contribution from the inter-membrane interferences; (2) the dashed curve in Fig. 3 gives the background for $I_o(\theta)$ which is the scattering intensity related to $I(Z)$; (3) $I(Z)$ is proportional to $I_o(\theta)\sin^2\theta$ with $Z=2\sin\theta/\lambda$, so that $|F_o(Z)|=I_o(\theta)^{1/2}\sin\theta$; (4) $F(Z)$ changes its sign at each zero point of $I_o(\theta)$. The validity of these assumptions will be discussed in the next section.

Fig. 4 gives $F(Z)=KF_o(Z)$ in e Å^{-2}, where K is the scale factor which will be determined below. An approximate electron density distribution $\varrho_o(z)$ was calculated in a relative scale by

$$\varrho_o(z)=2\int_{Z_{\min}}^{Z_{\max}} F_o(Z)\cos(2\pi Zz)\mathrm{d}Z\,. \qquad (3)$$

Here $Z_{\min}$ and $Z_{\max}$ define the region where the experimental data are available, so that $Z_{\min}=0{\cdot}009$, $Z_{\max}=0{\cdot}154$ in Å^{-1} for L and $Z_{\min}=0{\cdot}011$, $Z_{\max}=0{\cdot}165$ in Å^{-1} for LC. Referring to $\varrho_o(z)$, a trial step function $\varrho_{st}(z)$ is constructed with six parameters: the electron density levels $\varrho_1,\varrho_2,\varrho_3$, and the extensions x_1,x_2,x_3 of the terminal methyl trough, hydrocarbon core and uranyl-decorated head group, respectively. Here it should be noted that by definition $\varrho_o(z)$ is the difference of the electron density from that of water in a relative scale, but ϱ_i is the electron density itself. We have determined the optimum values of the parameters x_i and $\Delta\varrho_i=(\varrho_i-\varrho_w)/a$, where a is a constant for scaling, by searching the minimum of the residue R defined by

$$R\equiv\frac{\int_{Z_{\min}}^{Z_{\max}}|F_{st}(Z)-KF_o(Z)|\mathrm{d}Z}{K\int_{Z_{\min}}^{Z_{\max}}|F_o(Z)|\mathrm{d}Z}\,. \qquad (4)$$

Here $F_{st}(Z)$ is the Fourier transform of $\varrho_{st}(z)$ in a relative scale and K is the scale factor determined by

$$K^2=\int_{Z_{\min}}^{Z_{\max}}|F_{st}(Z)|^2\mathrm{d}Z\Big/\int_{Z_{\min}}^{Z_{\max}}|F_o(Z)|^2\mathrm{d}Z\,. \qquad (5)$$

Values of R were calculated for about 20 000 sets of the six parameters. The minimum value of R obtained was 0·24 for L and 0·27 for LC.

To express this in an absolute scale, $\varrho_{st}(z)$ is defined as the projection of electron density of one molecular unit, which means a uranyl-decorated lecithin molecule for L and a uranyl-decorated lecithin molecule plus 15/85 cholesterol molecule for LC. It is, however, not known whether the hydrocarbon chains are perpendicular to the membrane surface or are tilted. Therefore, the absolute value of $\varrho_{st}(z)$ was determined through solving the following equations for a and S, where S

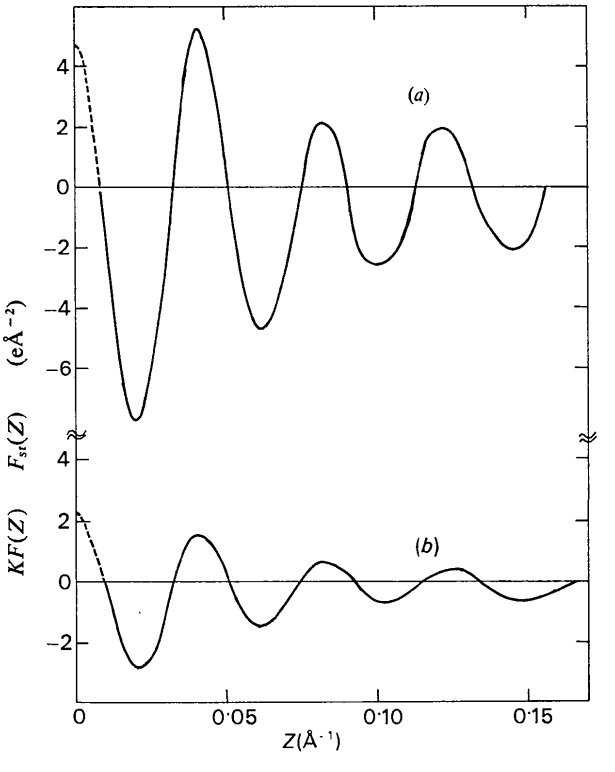

Fig. 4. Scattering amplitudes $F(Z)=KF_o(Z)$ (solid lines) and $F_{st}(Z)$ (dashed lines). (*a*) L; (*b*) LC.

is the average cross-sectional area of each molecular unit cut by a plane parallel to the membrane surface:

$$S\{a(\Delta\varrho_1 x_1+\Delta\varrho_2 x_2)+\varrho_w(x_1+x_2)\}=N_1\,, \qquad (6a)$$

$$S(a\Delta\varrho_3+\varrho_w)x_3=N_2\,. \qquad (6b)$$

Here ϱ_w is put equal to 0·335 e Å^{-3}, whereas $\Delta\varrho_i$ is known only in a relative scale at this stage. N_1 is the sum of the electron numbers of the two terminal methyls and two hydrocarbon chains and N_2 is the electron number of the head group bound by a uranyl ion. The value of S determined is 43·7 Å^2 for L and 49·5 Å^2 for LC. Finally obtained values of the parameters are $\varrho_1=0{\cdot}087$, $\varrho_2=0{\cdot}298$, $\varrho_3=0{\cdot}773$ in e Å^{-3} and $x_1=2{\cdot}0$, $x_2=18{\cdot}0$, $x_3=8{\cdot}0$ in Å for L; and $\varrho_1=0{\cdot}256$, $\varrho_2=0{\cdot}322$, $\varrho_3=0{\cdot}455$ in e Å^{-3} and $x_1=2{\cdot}0$, $x_2=16{\cdot}0$, $x_3=12{\cdot}0$ in Å for LC. By use of these values the final scale factor K was determined by equation (5). Now the electron density distribution $\varrho(z)$ is given by

$$\varrho(z)=K\varrho_o(z)+\varrho_w+\delta\varrho(z)\,, \qquad (7a)$$

$$\delta\varrho(z)=2\int_0^{Z_{\min}} F_{st}(Z)\cos(2\pi Zz)\mathrm{d}Z\,. \qquad (7b)$$

Fig. 5(*a*) and (*b*) gives $\varrho(z)$ together with $\varrho_{st}(z)$ for L and LC, respectively. The resolution of $\varrho(z)$ can be estimated by $1/Z_{max}$, which is 6·5 Å for L and 6·1 Å for LC. The autocorrelation functions are calculated based upon the following equations:

$$A(z)=A_o+\delta A(z)\,; \qquad (8a)$$

$$A_o(z)=2K^2\int_{Z_{\min}}^{Z_{\max}} |F_o(Z)|^2\cos(2\pi Zz)\mathrm{d}Z\,; \qquad (8b)$$

$$\delta A(z)=2\int_0^{Z_{\min}} |F_{st}(Z)|^2\cos(2\pi Zz)\mathrm{d}Z\,. \qquad (8c)$$

Fig. 6(*a*) and (*b*) gives calculated values of these functions for L and LC respectively.

Discussion

First we shall discuss the validity of the assumptions (1) to (4) on which our analysis has been based. As was demonstrated by Inoko *et al.* (1975), the bound uranyl ions cause repulsive forces between membranes, and inter-membrane distances seem to be very large (presumably more than 150 Å) in the dispersion. Therefore, effects of inter-membrane interferences (if there are such interferences) should appear mainly at very low angles. Careful examinations were made at the low-angle region around $2\sin\theta/\lambda\approx\frac{1}{150}$ Å^{-1} on photographs (not shown) taken by a Franks camera, but no indication of interference peaks was found. Also the autocorrelation function $A(z)$ should exhibit some peaks at large z if the inter-membrane interferences were appreciable. The $A(z)$ obtained shown in Fig. 6 is fairly flat for $z>60$ Å, supporting assumption (1).

Usually $\varrho(z)$ of a symmetric bilayer can be fairly well approximated by a pair of symmetric peaks, such as Gaussian functions separated by a distance D. This model gives the diffraction intensity $I(Z)$ zero points at $Z=(2n+1)/2D$ and maxima near $Z=n/D$ with $n=0,1,2,\ldots$. Also the scattering amplitude $F(Z)$ changes its sign at each zero point of $I(Z)$. In Fig. 3 the arrows indicate values of Z calculated by the above relations with $D=48{\cdot}8$ Å for (*a*) and 47·4 Å for (*b*). The actually observed minima and maxima lie close to these Z values. This fact suggests that the above model represents approximate features of our $\varrho(z)$ and that each minimum of the scattered intensity corresponds to the zero point of our $I(Z)$. This implies that the dashed

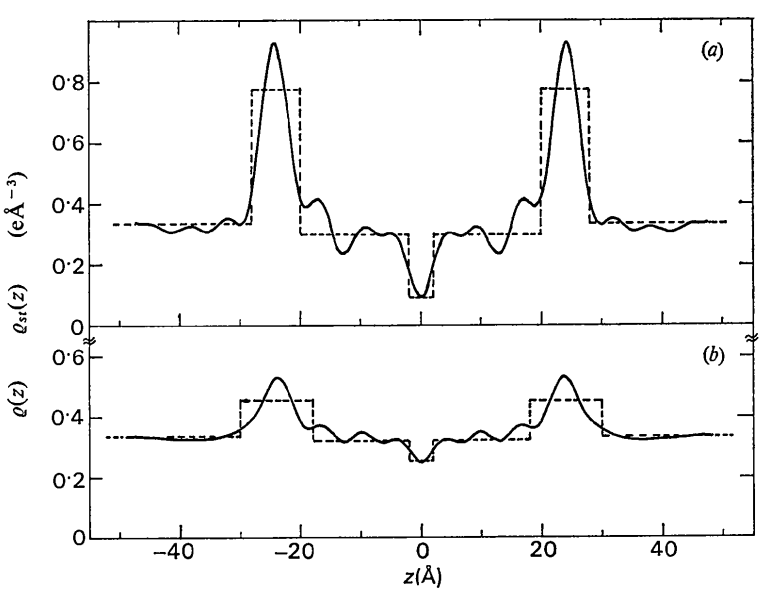

Fig. 5. Electron density distribution $\varrho(z)$ (solid curves) and $\varrho_{st}(z)$ (dashed curves). (*a*) L; (*b*) LC.

curve which passes through the minima of the observed intensity can reasonably be regarded as the background for $I_o(\theta)$ as postulated by assumption (2). Also it supports assumption (4) that our $F(Z)$ changes its sign at each zero point of $I_o(\theta)$. A further check on this phase assignment was made by calculating $\varrho_o(z)$ for all non-equivalent phase combinations ($2^6=64$) using equation (3). Density distributions which appear to be more reasonable than shown in Fig. 5, however, have not be found.

As is well known, the relation $I_o(Z)=I_o(\theta)\sin^2\theta$ is a good approximation for a random dispersion of membranes (Wilkins *et al.*, 1971). It can easily be proved that this relation holds even when there is a moderate preferred orientation as in the case of Fig. 2(*b*), if the length of the slit used for the densitometer tracing is small enough. It was 50 μm in our measurements and therefore assumption (3) does not seem to cause a serious error.

Table 1 of the article by Tardieu, Luzzati & Reman (1973) gives values of the cross-sectional area S and the tilting angle of the hydrocarbon chain with respect to the membrane surface in the dipalmitoyl lecithin bilayer at various water contents. The value of S (43·7 Å^2) obtained for our uranyl-decorated lecithin bilayer is closer to the value (42·7 Å^2) at low water content than the value (48·6 Å^2) at high water content given in their table. If we assume that this is caused by the change in the tilting angle, their table suggests that it is about 21° in L. According to van Deenen, Houtsmuller, de Haas & Mulder (1962), the cross-sectional area of cholesterol is 35 Å^2 in a monolayer at an air–water interface. If we adopt this value and assume that the tilting angle in LC is the same as in L, the value of S (49·5 Å^2) obtained in LC should be compared with $43{\cdot}7+35\times(\frac{1}{8}\frac{5}{5})=49{\cdot}9$ Å^2. These calculations suggest that our results for S are not unreasonable.

Several authors studied the electron density profile of dipalmitoyl lecithin bilayer. Luzzati, Tardieu & Taupin (1972) used the lamellar reflexions up to the 9th and obtained the density profile with a resolution of about 6·7 Å. Lesslauer, Cain & Blasie (1972) used the lamellar reflexions up to the 10th together with diffraction data from the dispersions and obtained the density profile with a resolution of about 6 Å. The result of the former was given in the absolute scale and is reproduced by the dashed line in Fig. 7 in comparison with our $\varrho(z)$ for L with a resolution of 6·5 Å. Agreement between them is fairly good except for the head group peaks. The length and density of the hydrocarbon core of our $\varrho(z)$ also agrees well with those reported for a fatty acid multilayer by Lesslauer (1974). Hitchcock, Mason, Thomas & Shipley (1974) have analysed the crystal structure of dilauroyl phosphatidylethanolamine and gave the electron density projection onto the normal to the bilayer at various resolutions. The density profile of the resolution of 5·5 Å (the curve (*b*) in Fig. 5 of their paper) suggests that in Fig. 7 the peak *a* of the dashed curve at $z=22$ Å corresponds to the PO_4 group. The peak *b* of the solid curve at $z=24$ Å seems to indicate UO_2^{2+}, judging from its height. All these results suggest that the uranyl ion binds to PO_4^- and sits slightly on the water side.

Fig. 5 shows that the uranyl-bound head group peaks are sharper and the terminal methyl trough deeper in L than in LC; this suggests that the structure of the bilayer in L is more ordered than in LC.

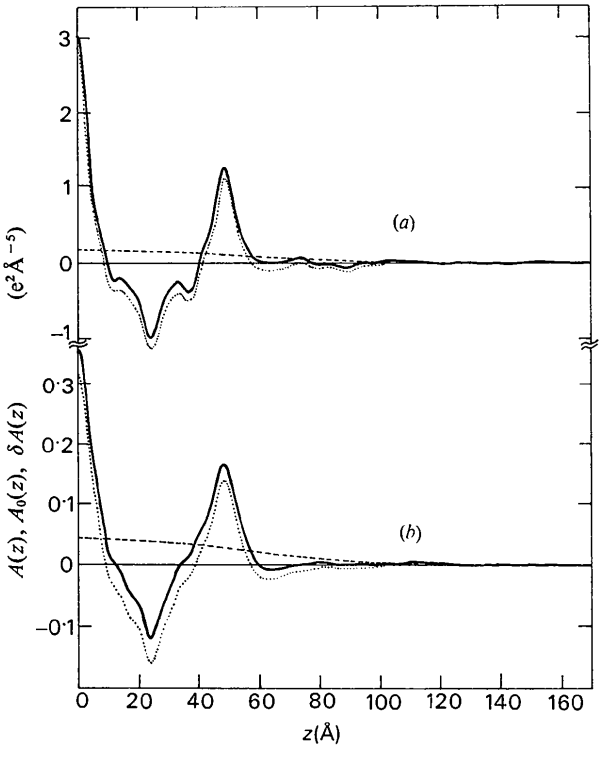

Fig. 6. Autocorrelation function $A(z)$ (solid curves), $A_o(z)$ (dotted curves) and $\delta A(z)$ (dashed curves). (*a*) L; (*b*) LC.

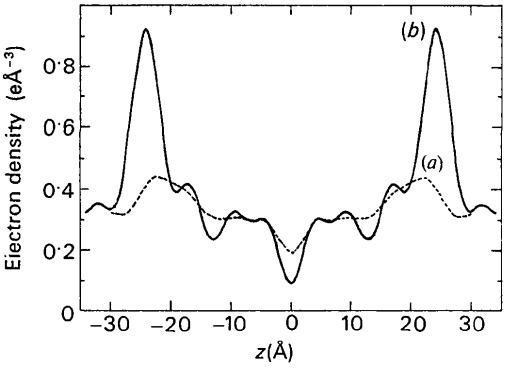

Fig. 7. Comparison of $\varrho(z)$ of L (solid line) with the electron density distribution reported by Luzzati *et al.* (1972) (dashed line).

Fig. 1 shows that the lecithin and lecithin–cholesterol bilayers are capable of binding about the same number of uranyl ions as lecithin molecules and also that cholesterol molecules do not affect the affinity of lecithin molecules for uranyl ions. Shah & Schulman (1967) studied the ionic structure of dipalmitoyl lecithin monolayers and proposed that one Ca^{2+} ion binds to two phosphate groups. Inoko *et al.* (1975) showed that cholesterol prevents the binding of Ca^{2+} ions to dipalmitoyl lecithin. The mode of UO_2^{2+} binding seems to be quite different from the case of Ca_2^{2+}.

Fig. 3(*a*) demonstrates that there is a bump in the background (the dashed curve) around $2 \sin\theta/\lambda \approx 0{\cdot}12$ Å^{-1}. The observations described in the *Experimental* suggest that this bump is a contribution from the scattered intensity in the vicinity of the X–Y plane in reciprocal space. As discussed by Inoko *et al.* (1975), the hexagonal unit cell usually assigned to the lipid membrane [$a \approx 4{\cdot}2.(2/\sqrt{3})$ Å] contains half a molecular unit of the head group. Such a situation can happen only when the arrangement of the head group is disordered, keeping the hexagonal symmetry in an averaged structure. One possible explanation for the bump is that it is caused by a local order in the arrangement of the uranyl-bound head groups of lecithin molecules.

References

DEENEN, L. L. M. VAN, HOUTSMULLER, U. M. T., DE HAAS, G. H. & MULDER, E. (1962). *J. Pharm. Pharmacol.* **14**, 429–444.

HITCHCOCK, P. B., MASON, R., THOMAS, K. M. & SHIPLEY, G. G. (1974). *Proc. Natl. Acad. Sci. U.S.* **71**, 3036–3040.

INOKO, Y., YAMAGUCHI, T., FURUYA, K. & MITSUI, T. (1975). *Biochim. Biophys. Acta*, **413**, 24–32.

LESSLAUER, W. (1974). *Acta Cryst.* B**30**, 1927–1931.

LESSLAUER, W., CAIN, J. E. & BLASIE, J. K. (1972). *Proc. Natl. Acad. Sci. U.S.* **69**, 1499–1503.

LUZZATI, V., TARDIEU, A. & TAUPIN, D. (1972). *J. Mol. Biol.* **64**, 269–286.

SHAH, D. O. (1969). *J. Colloid Interface Sci.* **29**, 210–215.

SHAH, D. O. & SCHULMAN, J. H. (1967). *J. Lipid. Res.* **8**, 227–233.

TARDIEU, A., LUZZATI, V. & REMAN, F. C. (1973). *J. Mol. Biol.* **75**, 711–733.

WILKINS, M. H. F., BLAUROCK, A. E. & ENGELMAN, D. M. (1971). *Nature New Biol.* **230**, 72–76.

Acta Cryst. (1976). B**32**, 1817

Affinement de la Structure de $NH_4NH_3CH_2COOHSO_4$ par Diffraction Neutronique

PAR SERGE VILMINOT ET ETIENNE PHILIPPOT

Laboratoire de Chimie Minérale C, Chimie des Matériaux, E.R.A. 314, *Université des Sciences et Techniques du Languedoc, Place E. Bataillon*, 34060 *Montpellier Cédex, France*

ET MOGENS LEHMANN

Institut Max von Laue–Paul Langevin, Avenue des Martyrs, 38000 *Grenoble, France*

(*Reçu le* 12 *novembre* 1975, *accepté le* 10 *décembre* 1975)

The crystal structure of ammonium glycinium sulphate has been refined by neutron diffraction using three-dimensional data collected on a four-circle diffractometer giving an R of 0·065. This resolution confirms the X-ray results concerning the heavy atoms and it has been possible to locate with precision the hydrogen atoms. A comparison between the two methods is made.

La structure du sulfate d'ammonium et de glycinium, $NH_4NH_3CH_2COOHSO_4$, a été réalisée par diffraction des rayons X, à la température ambiante (Vilminot, Philippot & Cot, 1974). Bien que cette étude ait permis de localiser les atomes d'hydrogène du motif, on peut douter de la précision et même de l'exactitude de cette détermination. Une étude complémentaire par diffraction neutronique devait donc nous permettre d'obtenir des résultats précis concernant les atomes d'hydrogène.

Partie expérimentale

Le sulfate double d'ammonium et de glycinium (en abréviation NGS) a été préparé par action du sulfate d'ammonium sur une solution sulfurique diluée de glycine suivant la réaction:

$$(NH_4)_2SO_4 + 2NH_2CH_2COOH + H_2SO_4 \rightarrow 2NH_4NH_3CH_2COOHSO_4 .$$

Des petits cristaux sont obtenus par évaporation lente de la solution et sont utilisés comme germes pour la croissance de monocristaux. Cette opération s'effectue dans une enceinte close, à double paroi, afin d'éviter de brusques variations de température du milieu réactionnel. La croissance cristalline est conduite par évaporation la plus lente possible d'une solution saturée dans laquelle est suspendu un germe monocristal-